

## Visualization and PDA Measurement of Spray inside a Thermostatic Expansion Valve

Ming Huo and Chia-Fon F. Lee\*

Department of Mechanical Science and Engineering  
University of Illinois at Urbana Champaign  
Urbana, IL 61801 USA

### Abstract

Thermostatic expansion valves (TEV) are expansion devices commonly used in air-conditioning system which involves the spray and atomization process of the refrigerant. The process was studied by introducing a valve with optical access. The break-up and atomization of the refrigerant were visualized near the outlet of the orifice under different feed conditions on micro-second scale. A Phase Doppler Anemometry (PDA) was used later to measure the size of individual droplets passing the location at the outlet of the orifice and provide drops size distribution (DSD) data. In addition, the effect of the feeding pressure was analyzed by measuring the DSD at same locations with different pressure value. Through this study, a better understanding of the expansion process inside the TEV is gained which will lead to better design and control optimization.

---

### Introduction

Thermostatic expansion valve (TEV) and electronic expansion valve (EEV) are commonly used for controlling the superheat of the refrigerant of the evaporator in air-conditioning systems, in order to increase the system efficiency. However, they exhibit poor control, either overfeeding or starving the evaporator, of mass flow rate of the refrigerant, also known as 'valve hunting'. This causes mal-distribution of the refrigerant in evaporator inlet circuits and reduces the efficiency of the entire system. Poor atomization of refrigerant inside the TEV is a major contribution to 'valve hunting', although the circuits and the accumulator also contribute to the problem.

The macro-features of the expansion valve and their impacts on the entire air-condition system, such as response time to the sudden superheat change in the evaporator and corresponding change in coefficient of performance (COP) have been investigated by a number of researchers [1, 2]. Various mass flow rate models related to the inlet and outlet conditions have also been developed [3, 4]. The microscopic features related to the expansion process inside the valve such as the spray structure and atomization characteristics are rarely found in open literature. Meanwhile, these microscopic features has been studied in internal combustion engine for decades applying techniques such as laser diagnostics and Phase Doppler Anemometry measurements and are capable in providing reliable results [5-8]. The application of these techniques to TEV is more challenging and is limited by the geometry of the TEV, since the expansion room is much smaller compared to the engine chamber, reducing the optical accessibility. Moreover, the high density droplets also reduce laser penetration. The objective of this study is to study the spray mechanism inside the expansion process using laser diagnostics and PDA to the TEV. The results allowed, on one hand, the visualization of the spray inside the TEV, and on the other hand, it help to shed light over the solutions of macro problems of refrigeration system, such as valve hunting.

In this study, the geometry of the poppet and orifice inside a stock TEV was directly duplicated and built into an adapter, which is then installed inside an optical chamber that allows for visualization. It should be mentioned that the results of this study can be applied to both TEV and EEV since valve control is not a concern and valve geometry is similar between TEV and EEV. Refrigerant R134a is used as the working fluid. The test section is mounted in a refrigerant loop, where all the feed conditions can be controlled and measured. The droplet breakup process is viewed using backlight illumination technique in microsecond scales. The droplet size and axial velocity in radial positions are measure by the PDA system in order to acquire the distribution map. Spray impingement is known to play a major role in the break-up process under certain conditions. By measuring the change in droplet size, its effect on the break-up process can then be studied.

### Experimental Apparatus and Procedure

#### System Configuration

---

\*Corresponding author

A schematic of the experiment facility is shown in Fig.1. The gear pump is used to provide the pressure head to R134a, a recycle bypass is then introduced to control the pressure of the fluid at the inlet of test section. The desired temperature of the fluid is controlled by the variac and the heater. Notice that the subcool degree of the refrigerant, defined as the degree below the saturation temperature, is settled once the pressure and the temperature are stabilized. After the test section, two-phase R134a is condensed in a plate heat exchanger by cooling water. A specific R134a receiver is mounted before the pump to avoid cavitations inside the gear pump. Within the test section, an adapter, machined to mimic the geometry of the inlet path of a commercial TEV, is mounted inside the chamber. A push rod is installed on a specially designed standoff, allowing vertical movement from outside the chamber. The needle is mounted on the top of the push rod and carefully aligned with orifice. In this way, open/close of the valve can be easily controlled by lifting up and down the push rod. The chamber has four side windows (Fig.2b). The position of the window is specifically chosen to meet the requirement of the PDA system.

#### a) Backlight Illumination Laser Diagnostics

Backlight illumination technique was employed to investigate the spray formation and breakup processes, permitting a qualitative study on the spray shapes and structure inside the expansion valve. Phantom Research v7.0 high-speed camera was used; an Oxford Lasers copper vapor laser was used as the light source. The frame rate was 10000 fps, which is equivalent to 10 $\mu$ s between each picture.

#### b) PDA measurement

The application of the LDA/PDA transmission system has been well documented [9, 10]. A Dantec Dynamics PDA system was used in this study to provide a quantitative analysis of the spray inside the TEV. Dantec P60 Flow & Particle processor was used for signal processing, while an Argon Ion Laser (Stabilite 2017) by Spectra-Physics was used as the light source. Spatial adjustments were done with a Dantec manual transverse system. In this setup, the spatial profiles of droplet size were measured by a one-dimensional PDA. The beam separation was 50 mm and the laser power was 900 mW at a wavelength of 514 nm per beam. The scattering light collection lens on the Dantec receiver optical system has a focal length of 310 mm. The receiver was positioned at a scattering angle of 70° to ensure only the first order refractions were collected.

### **Results and Discussion**

Geometric parameters included in the present TEV study were orifice diameter  $d$ , nozzle angle  $\alpha$ , nozzle length  $L$ , and poppet diameter  $D$ . (Table 1). The variation of the TEV opening controls the refrigerant flow area in the TEV, resulting in the change of the actual orifice diameter for flow restrictions. Fig.3. represents the cross-sectional flow area of the TEV, which varies with the up-and-down movement of the needle driven by the push rod. The linearity of the flow area to the EEV opening has been investigated and the detail can be found in Ref.3.

#### Spray pattern.

The inlet subcool degree is 5°C and the ambient pressure is 60 psi throughout this study. Fig.4. illustrated the spray pattern at different feeding pressure with different flow rates. At lower mass flow rates (5 g/s, 10 g/s), the droplets can be clearly seen with good laser penetration. At low inlet pressure, the spray angle is smaller, resulting vaporization pool formed in the vicinity of the poppet, where drops impinged on the surface of the pool and splashed away. Under high feeding pressure, the drops break-up is mainly due to the aerodynamic force and the dispersing cloud becomes discernable. Droplet impingement is reduced with the spread of the cone angle, implying complete atomization of most of the drops prior hitting the liquid pool. The change of the spray pattern with the increase of inlet pressure becomes less apparent at a higher flow rate (15 g/s), when large rainout droplets were seen in the downstream of the exit orifice, resulting in very low laser penetration. The spray with higher inlet pressure, somehow, is still more homogeneous from the picture.

In an attempt to further discuss the impact of the feeding conditions on the break-up regime inside the TEV, the impingement process is demonstrated on millisecond scale shown in Fig.5. Bulk liquid, marked with the red circle, can be observed at the orifice exit under low pressure feeding conditions. These large drops are not fully atomized prior to reaching the liquid pool, while secondary break-up occurs and the droplets are splashed away in certain directions. It is necessary to point out that the space in a typical expansion room in typical commercial TEVs is very small, on the order of 1 cm<sup>3</sup>. Therefore, the images taken in the chamber used in this study is suitable for practical usages. In real applications, the TEV often feeds into some kind of header before distributing the liquid refrigerant to each parallel circuit of the evaporator, where better atomization and lower droplet inertial forces could have the most benefit. A higher feeding pressure, which produces a much more homogeneous spray profile, is obviously a preferable choice from this point of view. Meanwhile, a liquid pool is undesirable as the liquid-phase refrigerant is accumulated and causes the aforementioned issues. Therefore, a configuration that provides more space for atomization and less likely in forming a liquid pool should be incorporated in future TEV design.

### PDA data

Drops size distribution (DSD) was obtained by sorting the droplets into 5  $\mu\text{m}$  sized bins, and the counts are normalized by the total number of droplets detected by the PDA receiver. DSD from tests performed at inlet pressure of 120 psi at two different flow rates is shown in Fig. 6. The measurement grid consisted of four radial positions from  $x = 3 \text{ mm}$  to  $x = 15 \text{ mm}$ , while the axial position of 2 mm from the orifice exit is kept although the experiment. The number density peaks in the region of 15-18  $\mu\text{m}$  and 26-30  $\mu\text{m}$  at flow rate of 5 g/s and 15 g/s respectively. An apparent difference could be seen between the DSDs recorded along the radial axis. The density peaks at larger radial distances shifted to lower drop size values for both flow rates, suggesting the smaller drops at the edge of the spray plume.

DSD data taken at the same distance from the nozzle, but at varying feeding pressures are shown in Fig. 7. The peak shifted towards smaller drop size at higher feeding pressure for both flow rates, which is consistent with the result from the image. The trend is less apparent at greater distance, though, which may be because the drops break up if there is enough space.

To verify the impact of the impingement, the particles were sorted by their velocity vector, and the distribution is shown in Fig. 8. for a refrigerant spray with a flow rate of 10 g/s and feeding pressure of 120 psi. The particles detected by the PDA with a negative axial velocity are categorized as “before impingement” and vice versa. At radial distance of 5mm, where is still close to the orifice exit, the particles after impingement contains only 8% of the total count, and appear to be smaller in size. This is not unexpected since there are large drops just coming out of the orifice and have not fully atomized as observed in previous figures. The particles after impingement at greater distance, however, contains 73% of the total count, and the size distribution appear to shift to bigger value, this can be partial evidence that the mechanical break up lead to smaller droplet than the secondary breakup caused by the impingement on a liquid pool, which should be investigated further in the future work.

### **Conclusions**

1. Spray patterns with the current TEV configuration at different inlet conditions were visualized. The images show that higher feeding pressure improves the atomization of the refrigerant through TEV by creating more homogeneous flow at the exit.
2. Low feeding pressure and higher flow rates tend to produce large droplets at the exit of the orifice, and secondary breakup caused by impingement is the dominant break-up regime. This suggests that the inner geometry of the TEV could be a concern for better atomization and preventing liquid pool.
3. Drops become smaller at the edge of the spray flume, shown by the DSD data. Also, smaller drops are observed at the same locations at elevated feeding pressure pressures, consistent with the image acquired.
4. The preliminary work suggests the potential of back light illumination and PDA technique in the research of TEV. A better understanding of the micro features of the expansion process is essential for an optimized valve design and operations conditions.

### **References**

1. Tassou, S.A. Al-Nizari, H.O. 1993. Investigation of the effects of thermostatic and electronic expansion valves on the steady-state and transient performance of commercial chillers. *International Journal of Refrigeration*. 16, 49—56
2. Ibrahim, G. A. 2001. Effect of sudden changes in evaporator external parameters on a refrigeration system with an evaporator controlled by a thermostatic expansion valve. *International Journal of Refrigeration* 24, 566—576
3. Park, C. Cho, H. Lee, Y. Kim, Y 2007. Mass flow characteristics and empirical modeling of R22 and R410A flowing through electronic expansion valve. *International Journal of Refrigeration* 30, 1401—1407
4. Ma, S. Zhang, C. Chen, J. 2005. Experimental research on refrigerant mass flow coefficient of electronic expansion valve. *Applied Thermal Engineering*. 25, 2351—2366
5. Reitz, R.D. 1990. A photographic study of flash-Boiling atomization, *Aerosol Science and Technology*, 12:3, 561—569
6. Lee, C.S. Reitz, R.D. 2001. Effect of liquid properties on the breakup mechanism of high-speed liquid drops. *Atomization Sprays* 11, 1—19
7. Blaisot, J.B. Yon, J. 2005. Droplet size and morphology characterization for dense sprays by image processing: application to the Diesel spray. *Experiments in Fluids* 39, 977—994
8. Lee, K. Reitz R.D, 2004 Investigation of spray characteristics from a low-pressure common rail injector for use in a homogeneous charge compression ignition engine. *Meas. Sci. Technol* 15, 509—519
9. Albrecht, H.E., 2003, Laser Doppler and Phase Doppler measurement Techniques (Springer, London, UK)

10. Al-Hakim, K. Wigley, G. Stapley, A.G.F 2006. Phase Doppler anemometry studies of spray freezing. *Chemical Engineering Research and Design* 84(A12):1142 —1151

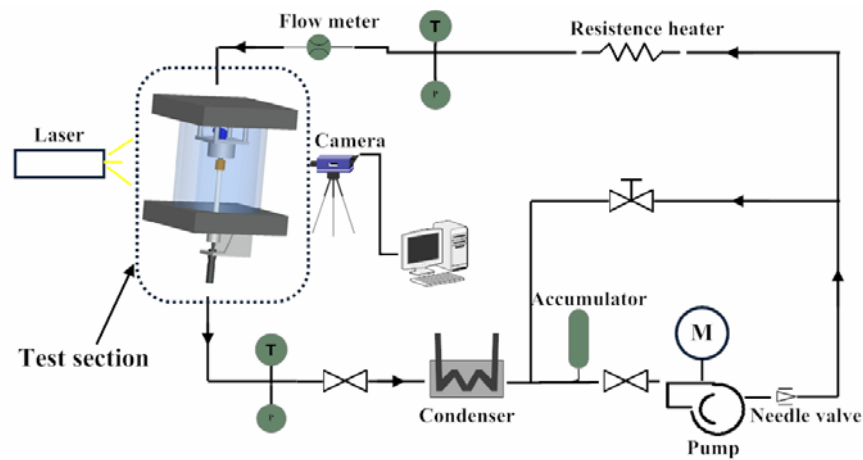


Figure 1. Experimental apparatus

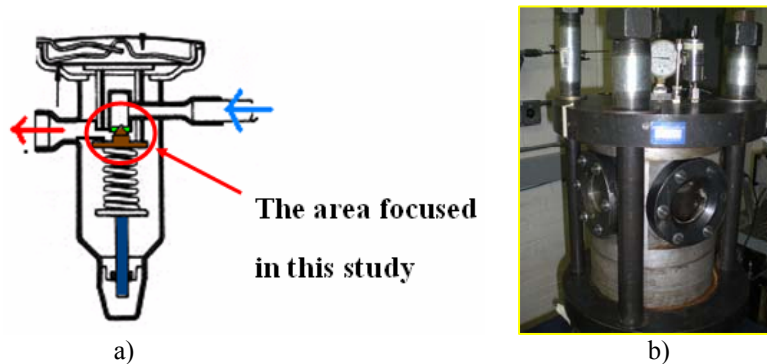


Figure 2. Test Section. a) Inner diagram of a commercial TEV. b) Chamber

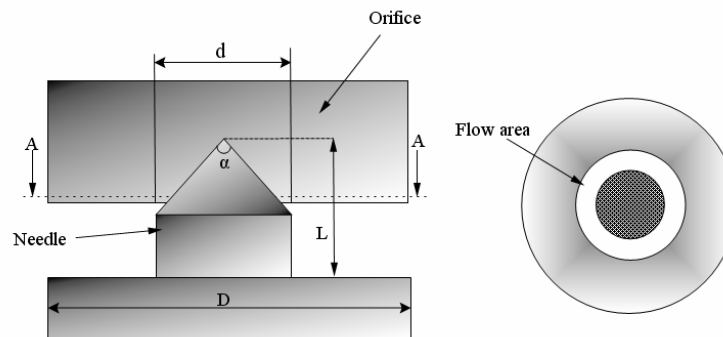
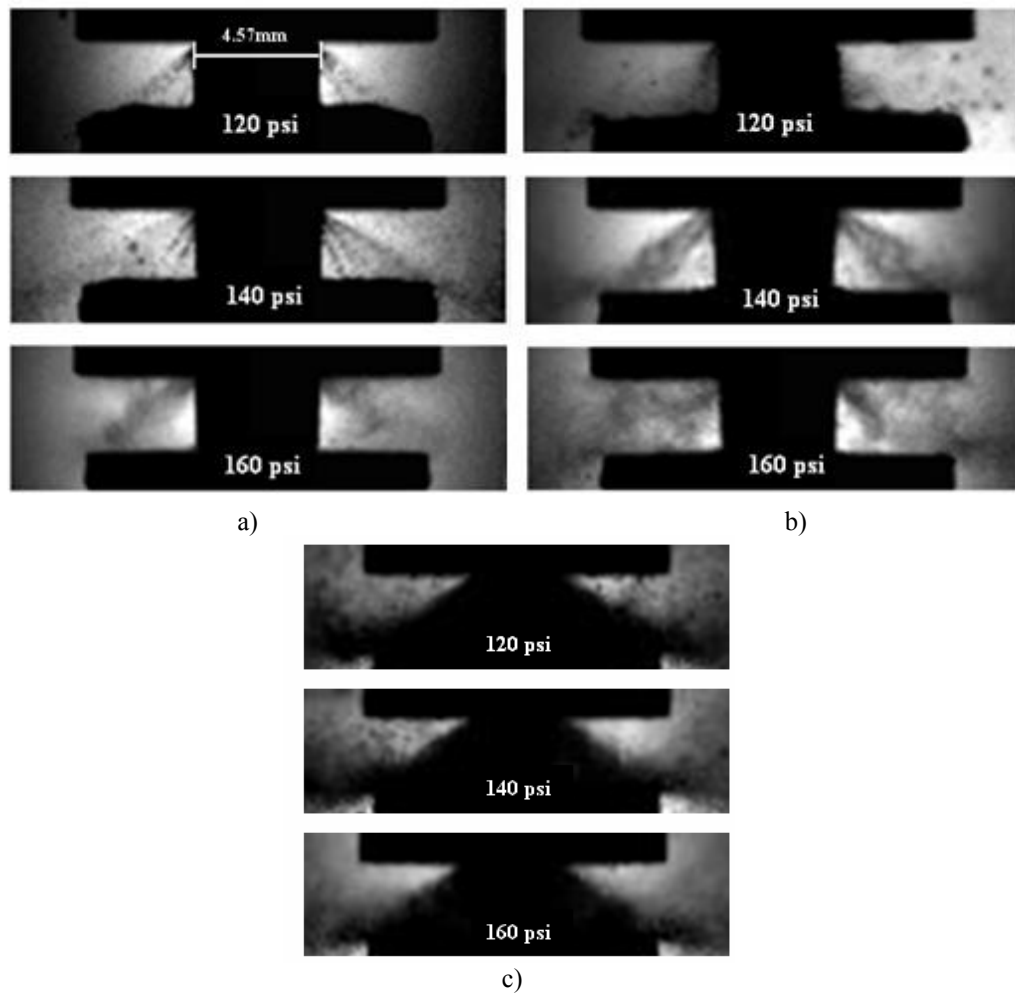


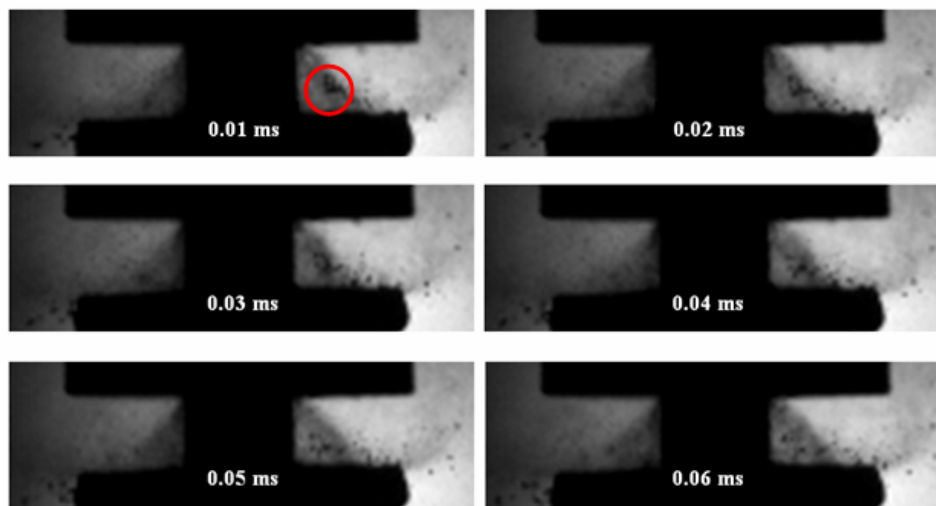
Figure 3. Front and cross-section view of the TEV

Table 1. Nozzle Characteristics

Orifice diameter $d$ (mm)	4.57
Nozzle angle $\alpha$	85
Nozzle length $L$ (mm)	5.13
Poppet diameter $D$ (mm)	14.32



**Figure 4.** Spray pattern at different inlet pressure with flow of a) 5 g/s, b) 10 g/s and c) 15 g/s



**Figure 5.** Evolution of the Impingement process of a refrigerant spray at  $p= 120$  psi with a flow rate of 10 g/s

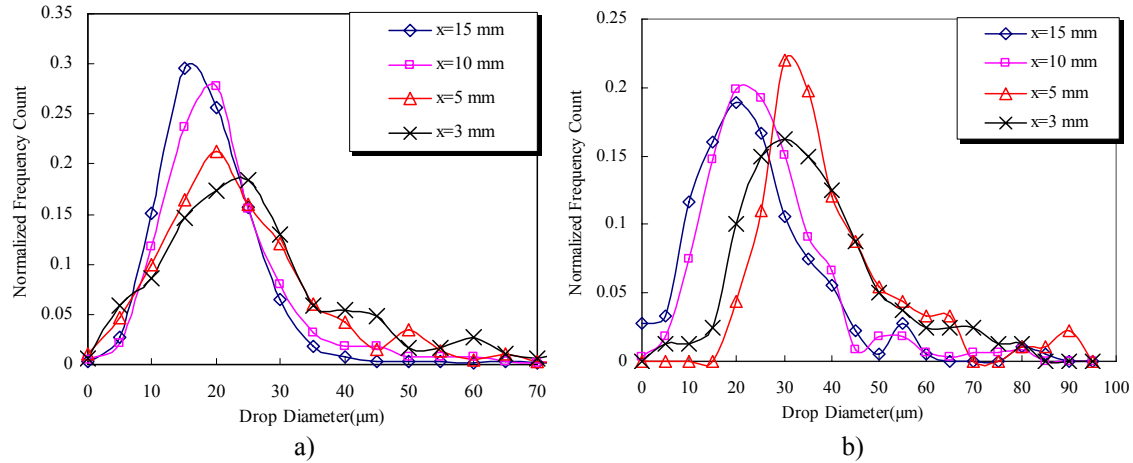


**Figure 6.** Drop size distribution (normalized against total number of detected particles) for a refrigerant spray at the inlet pressure of 120 psi and at various radial distances from the nozzle with a flow rate of a) 5g/s, b) 15g/s

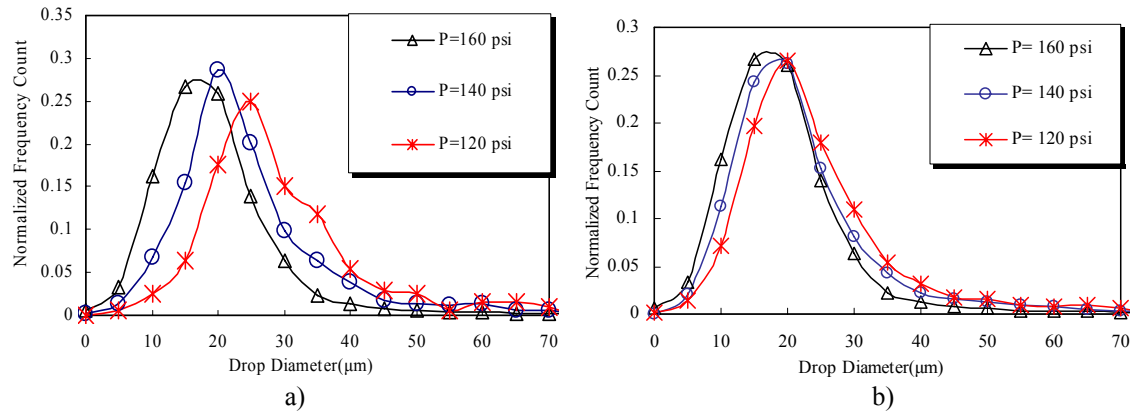


**Figure 7.** Drop size distribution (normalized against total number of detected particles) for a refrigerant spray at different radial distances from the nozzle a)  $x=5$  mm b) 15 mm, and at various inlet pressures with a flow rate of 10g/s

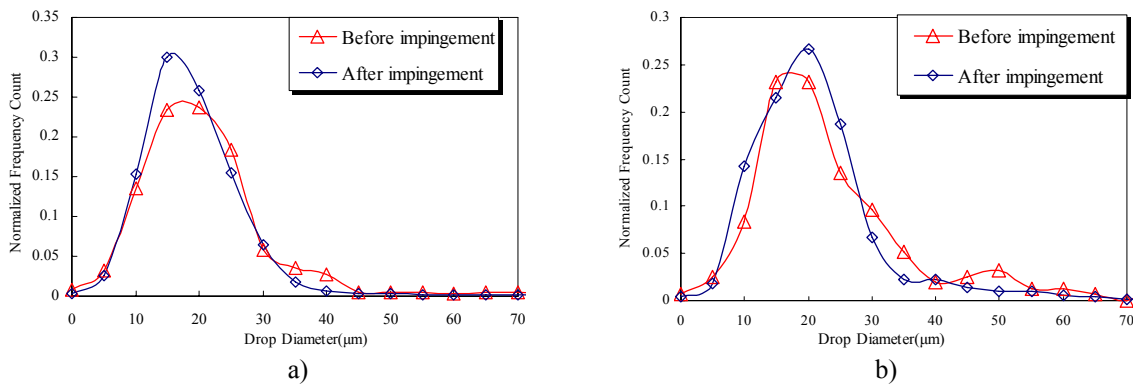


**Figure 8.** Drop size distribution (normalized against total number of detected particles) for a refrigerant spray before and after impingement at different radial distances from the nozzle a)  $x=5$  mm b) 15 mm, with a flow rate of 10g/s and feeding pressure of 120 psi.